LHCb-Memo-2000-80 RICH
6 September, 2000.

Monitoring, Alignment and Control of the RICH Detectors

C. D'Ambrosio[1], B. Franek[2], C. Gaspar[1], M. Laub[1], R. Lindner[1], F. Muheim[3], A. Papanestis[2], F.J.P. Soler[2,4].

[1]CERN, Geneva, Switzerland.
[2]Rutherford-Appleton Laboratory, Chilton, Didcot, Oxfordshire, United Kingdom.
[3]University of Edinburgh, Edinburgh, U.K.
[4]University of Glasgow, Glasgow, U.K.

Abstract

The physical quantities of the RICH detectors need to be monitored throughout the duration of the experiment to ensure that their performance remains within the design specifications. The present note describes all the physical quantities that need to be monitored and a description of possible devices that could be implemented to achieve the specified level of control. In addition, the angular resolution of the RICH detectors depends on an accurate alignment of the system. Proposals for this alignment procedure are described.

1. Objectives

The performance of the Ring Imaging Cherenkov (RICH) detectors of LHCb can be kept under control if one is able to monitor their physically relevant quantities. The ultimate performance of the RICH detectors depends on the angular resolution given by the reconstruction of Cherenkov rings in the photon detector planes. The main factors that affect this resolution are the refractive index of the gas and its wavelength dependence, the efficiency, quality and position resolution of the optical systems, the intrinsic resolution of the photon detectors and the accurate alignment of all the optical elements. The current note is a description of the quantities that need to be monitored and the alignment procedure that could be implemented to ensure that the angular resolution of the two RICH detectors and, hence, their particle identification capabilities, are kept within the design criteria.

2. Gas Monitoring

2.1 Gas Re-circulation System

The two gases for each of the RICH detectors (C_4F_{10} for RICH1 and CF_4 for RICH2) have different refractive indices and have to be monitored independently. Each RICH has its own closed circuit re-circulation gas system [1] to ensure the quality of the gas for each of the detectors. Figure 1 shows a schematic of the gas system for the RICH2 detector (RICH1 would have a similar system).

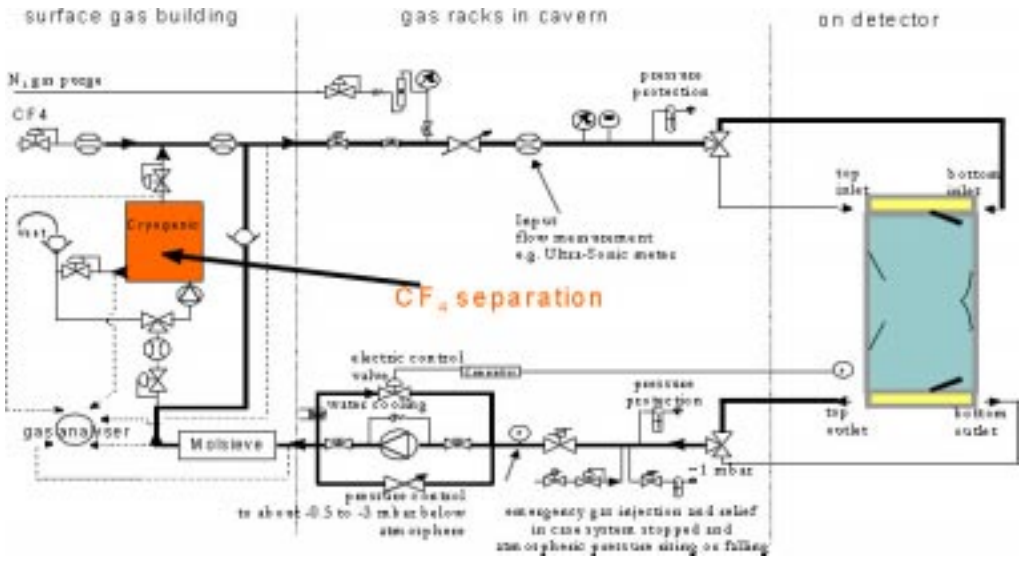

Figure 1: Gas circulation system for the RICH2 detector. RICH1 has a similar system.

The gas flows in a closed system, allowing 90% of the gas to be re-circulated, while the other 10% passes through the gas separation unit. Under normal operation, the gas flows through an inlet at the bottom of the vessel, with its flow monitored by an ultra-sonic flow meter (at a rate of approximately 1% of the volume per hour), and an outlet at the top of the vessel. In the case of removing the gas from the vessel and filling it with N_2, the valves are reversed and the inlet is at the top and the outlet at the bottom. The circuit has a pressure control system with two bubblers at the input and output. Three pressure gauges with a feedback control system, ensure that the gas remains between 0.5 mbar and 3 mbar below the atmospheric pressure. The gas flows through molecular sieves with pore diameter of 0.3 nm that allows the extraction of water vapour, which must remain with a concentration below 100 ppm.

Further purification is achieved by liquefying the gas in a cryogenic plant (see Figure 2) in order to separate it from its oxygen and nitrogen contaminants. The gases need to be cooled below their respective boiling points (C_4F_{10} at -1.9^oC and CF_4 at -128^oC at atmospheric pressure) and above those of oxygen and nitrogen, to extract these contaminants. The remaining liquid is stored in a storage tank and then can be heated to its gaseous phase for re-insertion into the closed system. The gas group will design a monitoring system to control all aspects of this cryogenic plant. The pressure and temperature of the liquefying vessel, the transfer to the storage vessel, the temperature of the heating element, the flow of liquid nitrogen used as a coolant and the flow of gas back into the main system are all the quantities to be monitored.

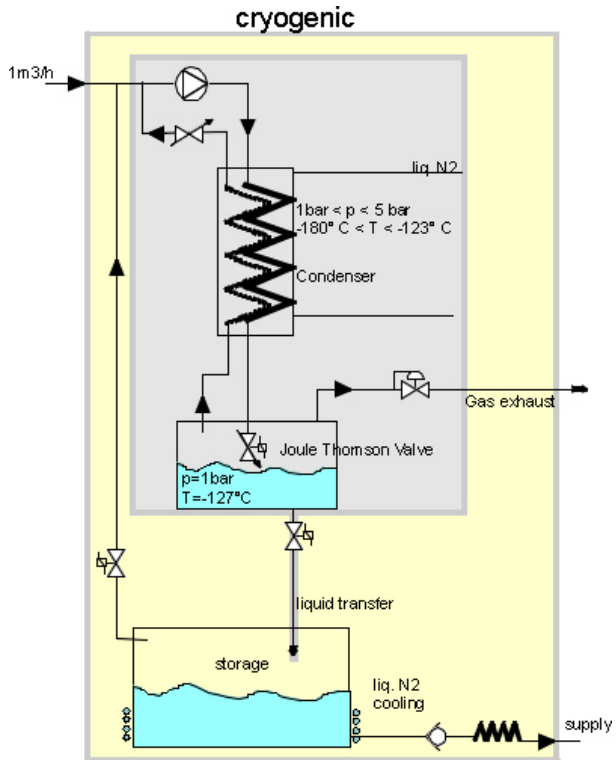

Figure 2: Cryogenic purification plant for the gas circulation system.

Oxygen and water can degrade the performance of the RICH by increasing the absorption in the far UV (mainly below 200 nm). Even though this problem is not as severe in the case of LHCb due to the spectral response of the photon detectors, traces of oxygen and water vapour in the gas mixture need to be controlled. The concentration of oxygen and water will be monitored in five positions in the gas system, as shown in Figure 1. These positions are at the input and output of the cryogenic plant, at the input to the main closed-circuit system from the cryogenic plant, at the outlet from the vessel, just before the molecular sieve and at the output of the molecular sieve. This is achieved with sensitive ceramic oxygen and water sensors that will be read out periodically. Even though this is not a critical parameter, the aim is to maintain the oxygen and water concentrations below 100-200 ppm.

Nitrogen is used as an inert gas to purge the system and its concentration will be maintained, under normal operating conditions, at about 1%. Since nitrogen can affect the refractive index, this concentration needs to remain constant, so it needs to be monitored continuously. This will be done with an ultrasonic sonar system (see Section 2.2).

The refractive index of the gas depends on its temperature and pressure. The pressure sensors at the input and output of the vessel will give a differential measurement of the pressure, with one device to measure the atmospheric pressure. In addition, temperature sensors inside the vessel will monitor the temperature of the gas. The small difference in hydrostatic pressure (~ 3 mbar) between the top and bottom of the RICH2 vessel (smaller for RICH1) can be corrected if necessary for the purpose of measuring the refractive index.

2.2 Refractive Index

2.2.1 Motivation

Knowledge of the refractive index of the gas is needed to be able to determine the particle velocity β once the Cherenkov angle has been measured. For C_4F_{10} the Cherenkov angle is about 53 mrad, with an expected resolution of 1.1 mrad, while for CF_4 the angle is 32 mrad with an expected resolution of 0.35 mrad [11].

One can measure the refractive index by selecting tracks with velocity β very close to 1 (for example electrons or high momentum muons) and measure the angle θ_c between the incoming track and the radius of the Cherenkov ring observed in the photon detector plane. The refractive index n (at the average wavelength given by the convolution of the Cherenkov spectrum, the absorption in the gas, the reflectivity in the mirrors and the quantum efficiency of the photon detector) is given by the following formula:

$$\cos\theta_c = \frac{1}{\beta n}.$$

For the experimental resolutions quoted above, one would be able to measure the convoluted value of *n–1* with an accuracy of ~ 4% for C_4F_{10} and ~2% for CF_4. Ideally, one would want to verify these values independently, with greater accuracy and as a function of wavelength, to ensure that the resolution in the refractive index does not degrade the performance of the RICH. The approach taken here is to measure the absolute value of the refractive index with a Fabry-Perot interferometer at selected times during the running period and to complement this measurement by monitoring deviations from these stable values in a continuous manner, with the aid of an ultrasonic sensor. These two will be described in the following two subsections in turn.

2.2.2 Fabry-Perot Interferometer

A Fabry-Perot interferometer was also used in the DELPHI RICH detector [3,4] to measure the refractive index of the gas. A sample of the gas is injected into a vessel containing a pair of semi-transparent mirrors (known commonly as an etalon) and interference fringes as a function of the pressure of the gas can be measured at a number of incident wavelengths (see Figure 3).

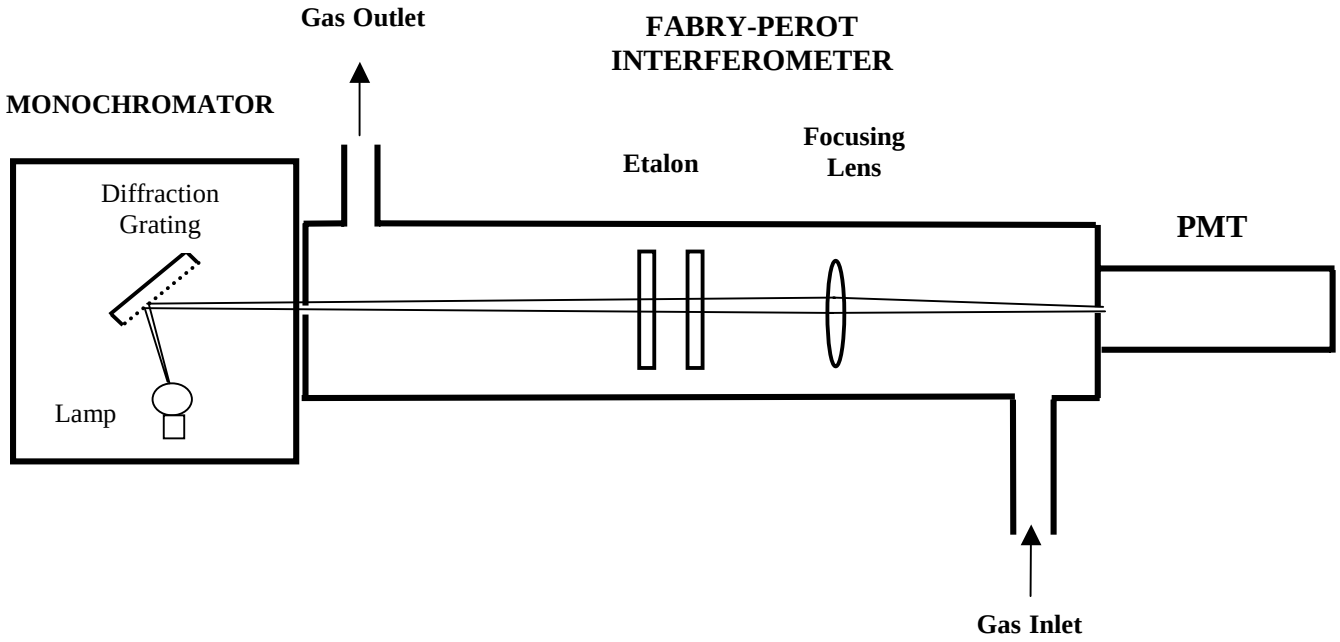

Figure 3: Schematic diagram of the Fabry-Perot interferometer for refractive index monitoring.

A monochromator can be used as the source of monochromatic light. Monochromators are commercially available and select a narrow band of wavelength by sending light from a lamp through a diffraction grating. The wavelength selection is achieved by changing the angle of the diffraction grating, only allowing light of a particular wavelength to pass through a collimator. Depending on the quality and cost of the monochromator, one can select wavelengths with a spectral bandwidth of approximately 1 nm, from the ultraviolet to the infrared.

The monochromatic light of wavelength λ passes through the etalon in the gas chamber, and is focused by means of a lens. In the DELPHI system, a collimator was placed at the focal plane and a photomultiplier detected the fraction of light from the central fringe that passed through the collimator. Alternatively, one could install a CCD camera at the focal plane and observe the interference fringes directly. The intensity of the detected light is given by the following:

$$I_{tot} = \frac{I_0 [T/(1-R)]^2}{1 + F \sin^2\left(\frac{2\pi d \cos\theta}{\lambda} n\right)}$$

where I_0 is the incident intensity, $F = 4R/(1-R)^2$ is the finesse, R, A and $T = 1-R-A$ are the reflectivity, absorbance and transmittivity of the mirrors, d is the distance between the mirrors and θ is the angle of incidence of the light. The pressure and temperature of the gas are also monitored in the chamber. As the pressure P of the gas is increased, one counts the number of interference fringes N(P) from vacuum to a final pressure. The refractive index as a function of pressure is then given by:

$$n(P) - 1 = \frac{\lambda}{2d} N(P)$$

DELPHI achieved an accuracy of the order of 1% in the measurement of $n-1$ [3,4]. This is better than the measurement of the refractive index that can be achieved by using ultra-relativistic particles. By employing this technique, we can make sure that the error in the determination of b is not degraded significantly by the resolution in the refractive index. In addition, the refractive index as a function of wavelength can be fed into the simulation program for a more reliable determination of the performance of the RICH.

These measurements can be time consuming so one would not carry them out continuously. They could be performed at given time intervals (for example, once a month). A complementary monitoring can be performed with an ultrasonic sonar sensor, to measure deviations from the absolute value of the refractive index measured by the Fabry-Perot.

2.2.3 Ultrasonic Sonar

Variations in the refractive index due to increased concentrations of nitrogen in the system can be monitored continuously with the use of an ultrasonic sensor. Such a device has also been successfully used in the DELPHI detector [2]. The principle of operation is to measure the velocity of sound in the gas at a frequency (49 kHz) where the following formula is valid:

$$v = \left(\frac{\gamma R \mathrm{T}}{\mathrm{M}}\right)^{1/2}$$

with $\gamma = C_p/C_v$, C_p and C_v the specific gas constant at constant pressure and volume respectively, T the temperature, R the ideal gas constant and M the molecular weight of the gas. Any deviations from the nominal velocity of sound for a pure gas (either the C_4F_{10} or the CF_4) would be symptomatic of trace contaminants in the gas that would affect its refractive index. The measurement of the velocity of sound determines the concentration of the trace contaminant of gas in a binary gas mixture. The sound velocity as a function of the binary gas mixture is calibrated initially for the gases that would be mixed with the radiators (either N_2 or Ar).

A Polaroid 6500 transducer[1] was used in DELPHI as both the loudspeaker and the microphone. A schematic of a possible arrangement is shown in Figure 2. The gas is introduced into a cylinder, with the transducer at one end and a reflector at the other end. The difference in time between the initial sound pulse train and the reflected signal determines the speed of sound in the column. The velocity of a pure sample of $C_4 F_{10}$ has been measured to be 101.145 m s^{-1} [2], and the equivalent velocity for CF_4 still needs to be measured. Any impurities in the gas manifest themselves by a modification of the molecular weight of the gas and hence by a change in the velocity. By maintaining the velocity of sound measurement within a tolerance window, we ensure that the refractive index does not deviate significantly from its nominal values.

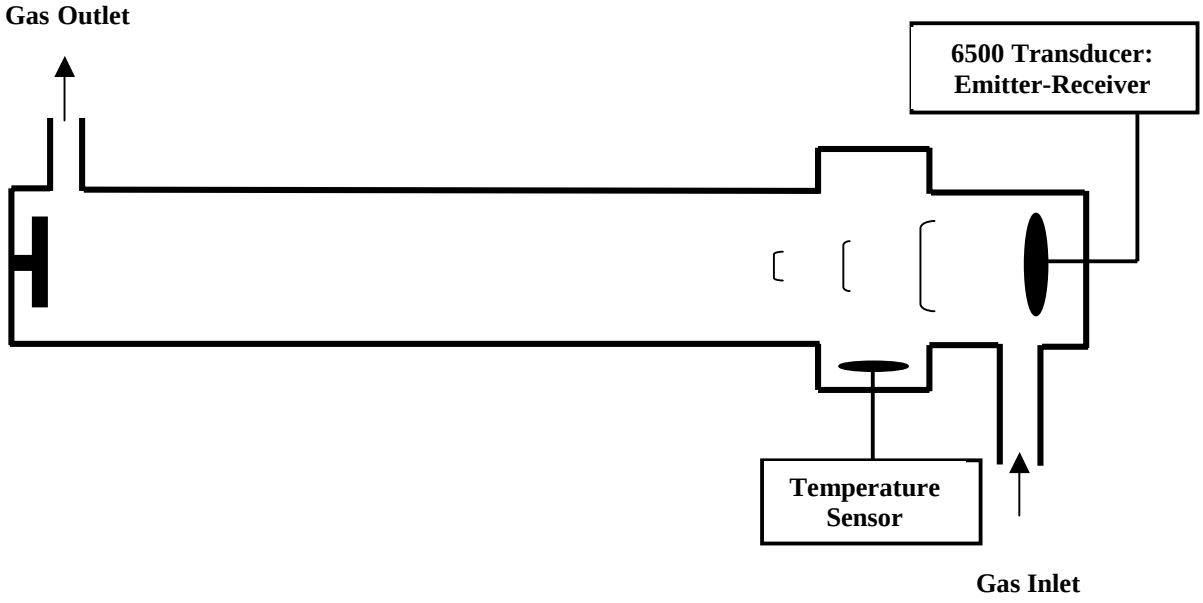

Figure 2: Schematic diagram of the ultrasound sonar system for gas purity monitoring.

2.3 Transparency of the Gas

The photon yield of the RICH depends very strongly on the absorption characteristics of the gas in question. Water and oxygen have absorption bands between 160 nm and 190 nm. Since the photon detectors are insensitive to light below 200 nm, these should not pose a problem for the

[1] Used as the range finder of an auto-focus camera.

efficient operation of the LHCb RICH systems. However, it is still desirable to monitor the transparency of the gas in the active region (between 200 and 800 nm), in case traces of other contaminants have absorption bands in that spectral region. The operational experience of DELPHI [5] shows that unexpected contaminants can degrade the transparency of the gas[2]. Monitoring of the absorption characteristics below 200 nm can also be used as an independent diagnostic tool to determine the concentration of water and oxygen in the gas.

It is proposed that a monochromator be used also to measure the absorption characteristics of the two gases in question (CF_4 and C_4F_{10}). Two cells with a variable length could be arranged perpendicular to each other (see Figure 4). A semi-transparent mirror (CaF_2), tilted at 45^o, partially reflects the light into one cell and the remaining light is focused onto the other cell. A photomultiplier with a wavelength shifter, to achieve sensitivity in the UV, is set up to measure the photon signal. Runs with the cells in vacuum would be used to achieve the absolute normalization. Alternatively, one can vary the length of the cells to achieve a relative measurement that can be used to obtain the attenuation length of the gas. These measurements are particularly important when a new batch of gas is in place or at the beginning of a run when the whole system is new. The experience gained at DELPHI suggests that the gases are clean from trace impurities after typically one week of running through their recirculation gas system [5].

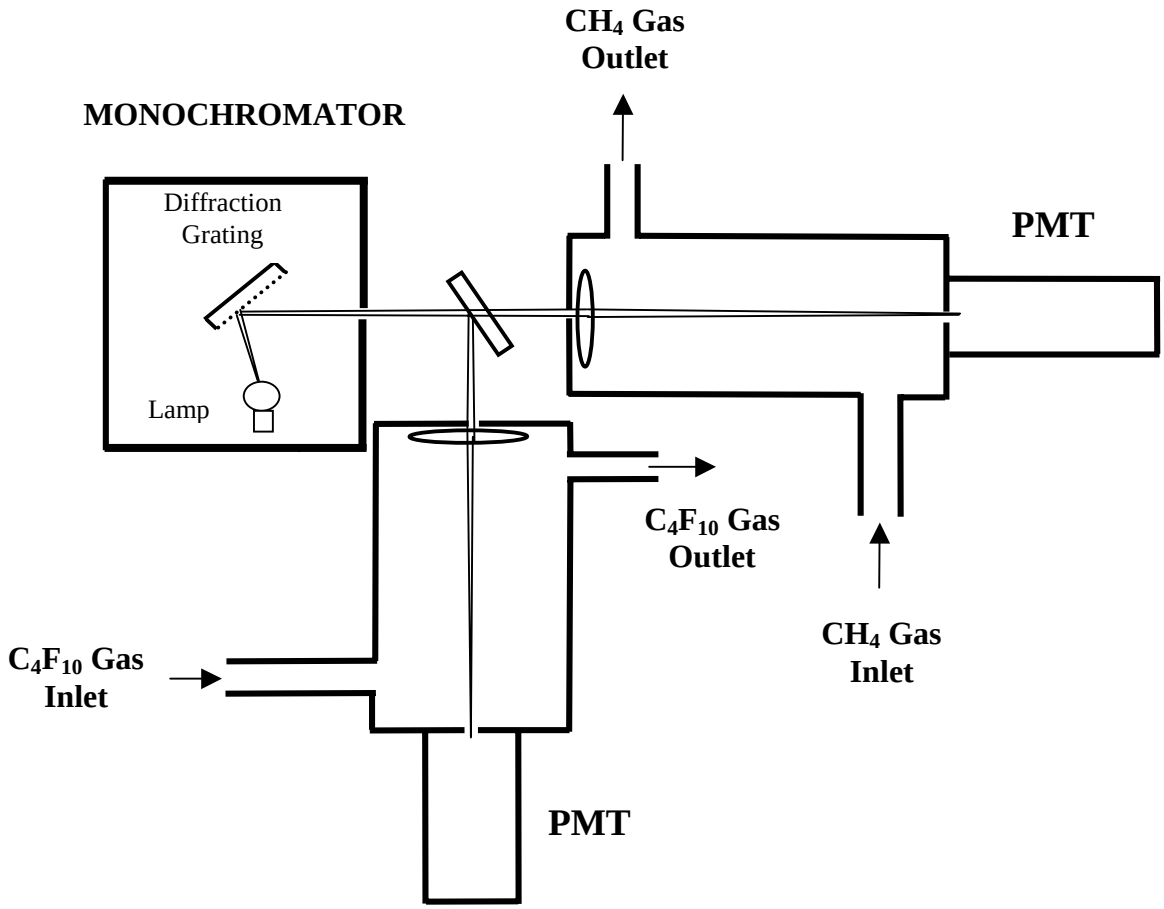

Figure 4: Monochromator for transparency measurements of both gas systems.

[2] Incompletely fluorinated molecules $C_nH_xF_{2n-x}$ and polymers can cause unwanted absorption bands.

3 Mechanical Monitoring

The angular resolution of the RICH depends on the mechanical stability of the frame, the mirror mounts and the photon detector mounts. Relative movements of these detector elements can cause a degradation in the position sensitive information. Inexpensive semi-transparent position sensitive silicon sensors [6-8] have been developed for the optical multi-point alignment system of the ATLAS muon spectrometer. The concept consists of using laser beams that act as alignment references, which are detected by the semi-transparent optical sensors at different alignment stations.

A silicon laser diode (λ = 690 nm) is used as the light source that feeds an array of single mode optical fibres. Commercially available fibre splitters can supply all the available transmission fibres. The laser light is transported via the optic fibres to each of the alignment stations where collimator optics are mounted (see Figure 5). The collimator produces a diffraction limited Gaussian laser beam with a 2-3 mm width over distances between 10-20 m. This allows one to install the fibres with their collimator optics in the inaccessible detector areas, while the laser remains accessible in the experimental control area.

The sensors consist of a thin film (~1 μm) of hydrogenated amorphous silicon (a-Si:H) deposited between two layers of indium-tin oxide (ITO) of ~100 nm thickness on a 5 mm glass substrate. The two layers are segmented into 64 strips, with a pitch of 312 μm, orthogonal to each other. The top layer acts as a Schottky diode with a 3 V bias voltage and the bottom layer is the Ohmic contact. The active area of these sensors is 20 x 20 mm^2. The laser light absorbed in the amorphous silicon induces currents in the two strips, thereby giving a measurement of the vertical and horizontal profile of the beam. The fit to the beam profile can achieve very good spatial resolution of ~ 1 μm. The transmittance of these sensors is above 80% at 690 nm. They can operate at high magnetic fields due to the very low Hall mobility of amorphous silicon and they show excellent radiation performance due to the thin layer and the amorphous structure that requires no doping.

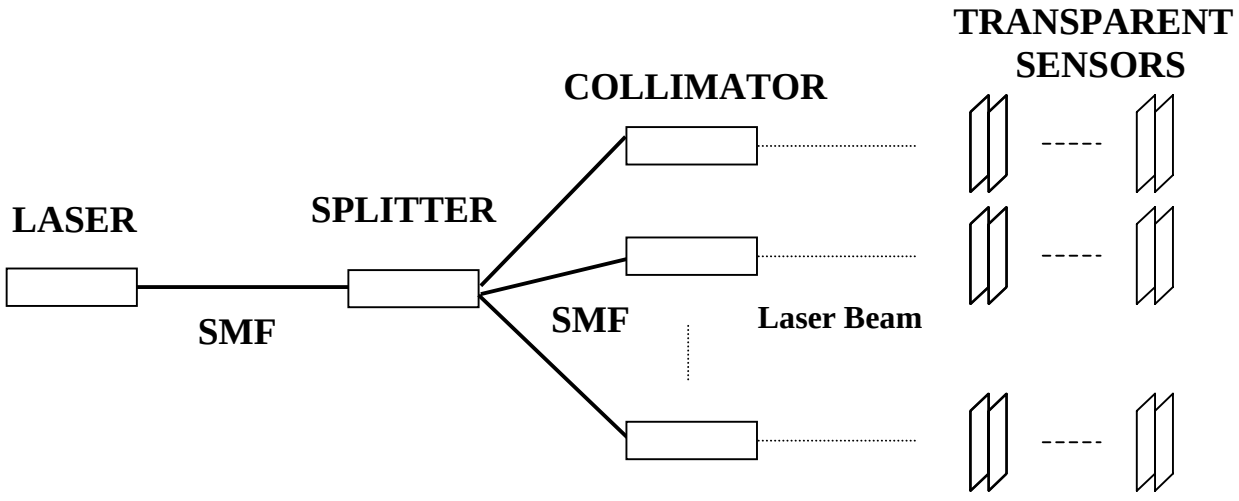

Figure 5: Distribution of the single-mode fibres (SMF) that feed a multi-point laser alignment system with transparent sensors.

The readout electronics consist of an analog multiplexer, amplified by a current voltage transformer, digitised by an 11-bit ADC and stored in a local memory that is read out. These sensors, with their associated electronics, were used to monitor the relative movements of each of the silicon detector planes of the NOMAD-STAR vertex detector [9], where they operated over two years without any problems, achieving a resolution of 1.5 μm.

It is proposed that 4 pairs of silicon sensors (a pair of sensors allows redundancy in the measurement) be mounted on top of each of the mechanical frames, as shown in Figure 6 to measure the stability of the support structures. The optic fibre and collimator is mounted on an independent structure and the beam of light is made to pass through the first two pairs of sensors. Two mirrors at each of the corners of the structure redirect the beam towards the other two pairs of sensors. The laser can be fired at regular periods (for example, once an hour) to monitor the stability of the mechanical support structures of the RICH.

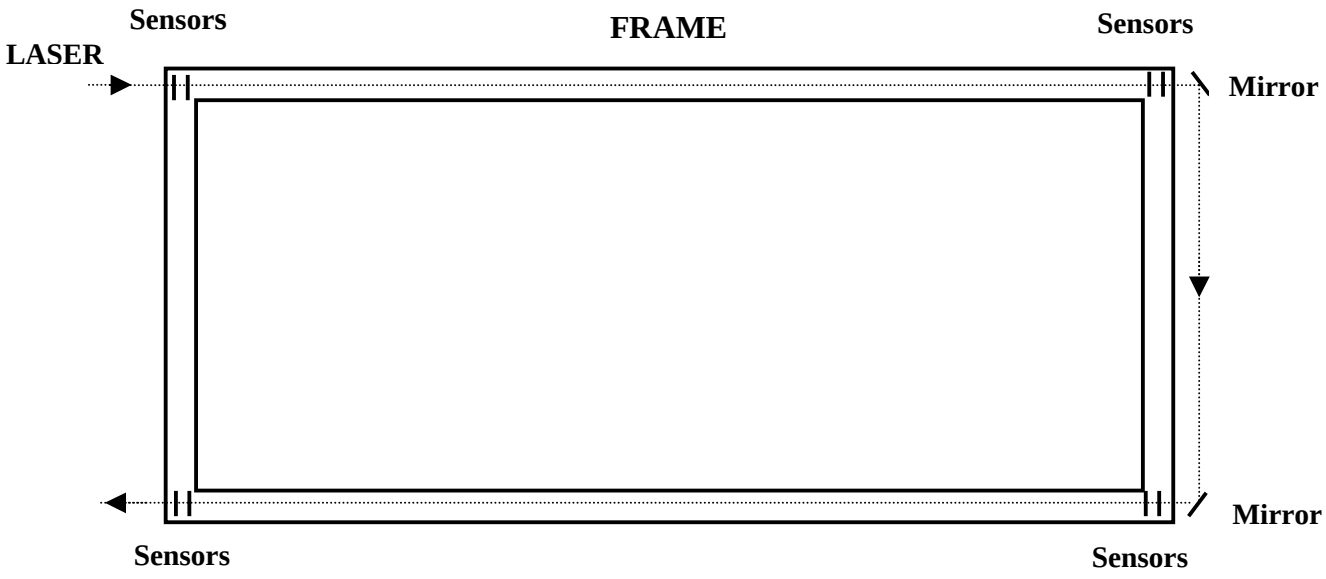

Figure 6: Position of silicon sensors for stability monitoring of support frames.

Alternatively, one could set up such sensors on the back of each of the mirrors of the two RICH detectors and on the photon detector support frame. This would monitor the relative movement of the mirrors and the photon detector plane with respect to the support frame. However, such relative movements can also be monitored by using a comprehensive alignment system, as will be discussed in Section 6.

4. Electronics Monitoring

There are a number of monitoring tasks that need to be carried out with respect to the photon detectors and electronics. There are four sets of voltages that need to be controlled and monitored for the photon detectors:

- high voltage of the photon detector tubes;
- voltage across the focusing elements;
- bias voltage for the pixel detector; and
- low voltage for the detector electronics.

The high and low voltages will be provided by appropriate computer controlled modules. A user-friendly interface will be designed for setting the individual voltages. The voltage and current values, as well as the leakage current from the pixel detectors, will be monitored continuously.

The binary readout electronics relies on a discriminator to select a valid signal for all the pixels in two tubes. The discriminator level will be set from the slow control system and its value will also be monitored. In combination with a light source (see Section 5), this allows one to carry out threshold scans at the beginning of each data-taking period to determine the pedestal, noise and one photoelectron levels of each of the pixels in each photon detector. The actual running thresholds can then be set at the ~2000 electron level.

One can also test the electronics chain by sending test pulses to each of the electronics channels and measuring the output response. This task would be carried out within the normal data-flow of the RICH readout, as separate calibration runs. However, the size of the test pulse for the front-end chip will be set from the electronics monitoring and control system.

5. Photon Detector Monitoring

At the beginning of each run, it is useful to have a fast tool to verify that each of the photon detectors is working. This can be achieved with a light pulser system installed inside the RICH vessel. There are a number of options for the light source. These could be an LED, a laser source, a xenon lamp with filters or a monochromator. The main aim is to illuminate the whole face of the photon detector plane with light, and observe the response of each of the detectors. This allows one to quickly identify potential problems with the tubes themselves, or with the electronics. Any faulty channels can be changed before the closure of the vessel. Furthermore, this light source can be pulsed at given times to monitor the number of dead channels in the system, during the data taking period. A schematic diagram is shown in Figure 7.

The long-term stability of the photon detectors is of paramount importance to ensure that the performance of the RICH does not degrade with time. The quantum efficiency and average photoelectron yield for each of the photon detectors can be determined with the above-mentioned light source. After pulsing with the light source, the efficiency η of a valid signal (if $\eta < 1$) can be related to the number of photoelectrons N_{PE}, under the assumption of Poisson statistics, by the following formula:

$$N_{PE} = -\ln(1-\eta).$$

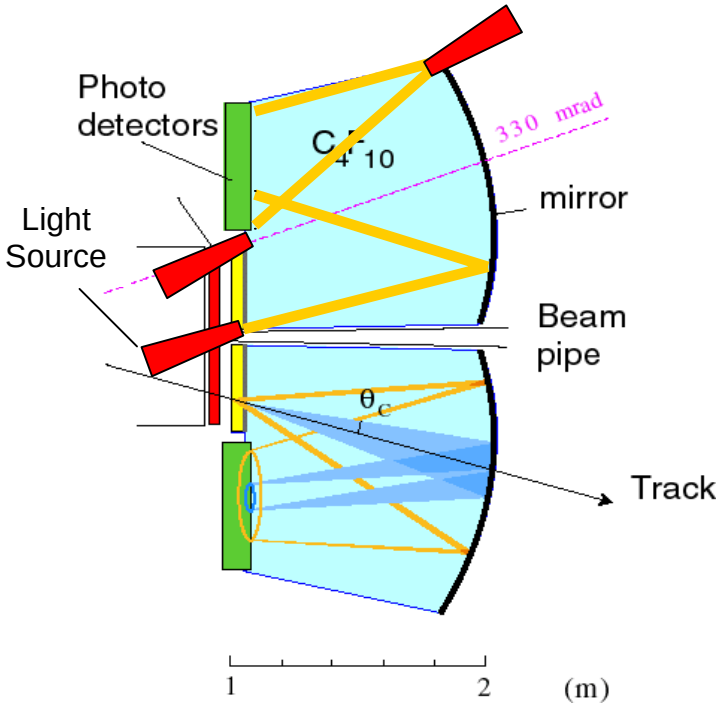

Figure 7: RICH1 detector with test light source.

Fixed runs throughout the data-taking period can measure the quantum efficiency as a function of time and as a function of incident wavelength.

The magnetic field can severely degrade the performance of the photon detectors. For this reason, we would also envisage monitoring the field at the position of the photon detector plane with a series of Hall probes that would also be read out by the general monitoring system.

6. Alignment

The alignment of the photon detector planes is crucial to ensure the angular resolution of the RICH detectors. The experimental aim is to have an angular resolution of 0.35 mrad in RICH 2 and 1.1 mrad in RICH 1 [11]. These resolutions comprise a component due to the uncertainty in the emission point as the track traverses the RICH detector (0.21 mrad for RICH2 and 0.54 mrad for RICH1), the chromatic error due to the wavelength dependence of the refractive index (0.22 mrad in RICH 2 and 0.54 mrad in RICH 1) and the spatial resolution due to the pixel size (0.18 mrad in RICH 2 and 0.72 mrad in RICH 1, assuming pixels 2.5x2.5 mm^2). Any alignment errors would degrade the pixel resolution of the photon detectors, so the experimental aim is to maintain such an alignment error below 0.1 mrad.

Ultimately, the relative alignment of the mirrors with respect to the photon detectors can be achieved by reconstructing Cherenkov rings for $\beta=1$ particles and comparing the differences between the reconstructed photons with respect to the expected position of the photons if the mirrors were perfectly aligned. This approach has been used successfully for other experiments

(see for example [12]), but it relies on an accurate survey of the initial positions of the mirrors before this iterative procedure converges successfully. An additional complication associated with this procedure relies on the ambiguity in determining from which mirror segment the photons originate. This problem is particularly severe in the case of RICH 2, where each photon originates from two reflections, one from a spherical segment and the other from a flat mirror segment. Only photons that are unambiguously associated with two mirror segments can be used for the alignment.

6.1 Survey of mirror and detector components

The first step towards providing an alignment procedure is to accurately survey the positions of the mirrors and photon detectors. The strategy to be adopted for the case of RICH 2 will consist of mounting all the mirrors on the mirror support plates in clean laboratory conditions. In the current design there are two flat mirror planes, consisting of 20 rectangular mirrors each plane, and two spherical planes, with 28 hexagonal and half-hexagonal segments each plane.

Access to the mirror support mounts is possible under clean laboratory conditions. All the mirrors will be mounted on the support plate and their relative positions and tilts will be determined with the help of the CERN based surveyor teams which can determine the relative position of the mirrors with an accuracy of less than 1 mm. The plates are then installed within the general RICH 2 frame and the position of these frames can also be determined with the surveyors. The positions of the detectors inside their own structure will also be surveyed and mounted on the RICH 2 mechanical frame. All the survey information will give a relative position error of each of the optical elements of approximately 1 mm. This would translate in a Cherenkov ring reconstruction error of ~1-2 mrad, which is clearly insufficient for the requirements of RICH 2.

For the case of RICH 1, the whole detector will be built in the laboratory before installation in the pit. This includes the photon detectors in their structure and the mirrors on their mounting structure. The relative positions of the photon detectors with respect to the mirrors will also be surveyed by a surveying team. Assuming a similar position accuracy of 500 μm, this would be equivalent to a Cherenkov angle resolution of ~1 mrad.

6.2 Alignment with data

One method of improving the errors incurred by the mirror misalignments is by using relativistic tracks ($\beta = 1$), which could be high momentum muons, electrons or hadrons. The reconstructed Cherenkov rings are compared to the ideal rings that would be formed if the mirrors and detectors were ideally aligned. This procedure is more complicated for the case of RICH 2 where two mirror reflections have to be taken into account if one wants to align both planes of mirrors. This procedure is being used in the alignment of the HERA-B RICH detector [12], and has been investigated in a preliminary manner in the context of the RICH 2 of LHCb [13].

The measured Cherenkov angle is defined as the angle formed between the direction defined by the photon hit on the detector and the direction defined by the particle path (Figure 8). The tilt

angle, tilt orientation, position of the mirrors and radius of curvature are all possible causes of errors for the accurate reconstruction of the Cherenkov angle. If the reconstructed angle is θ_c^{rec} and the expected angle is θ_c^{exp}, any misalignment in the mirror segments with respect to the photon detectors is observed by measuring the difference between the two angles as a function of the reconstructed azimuthal Cherenkov angle ϕ_c^{rec}. Since the centre of the Cherenkov ring is displaced with respect to the expected position (see Figure 8), the difference in the Cherenkov angles has the following dependency:

$$\theta_c^{rec} - \theta_c^{exp} = A \cos (\phi_c^{rec} - \phi_0) ,$$

where A and ϕ_0 are parameters that arise from fitting the previous function.

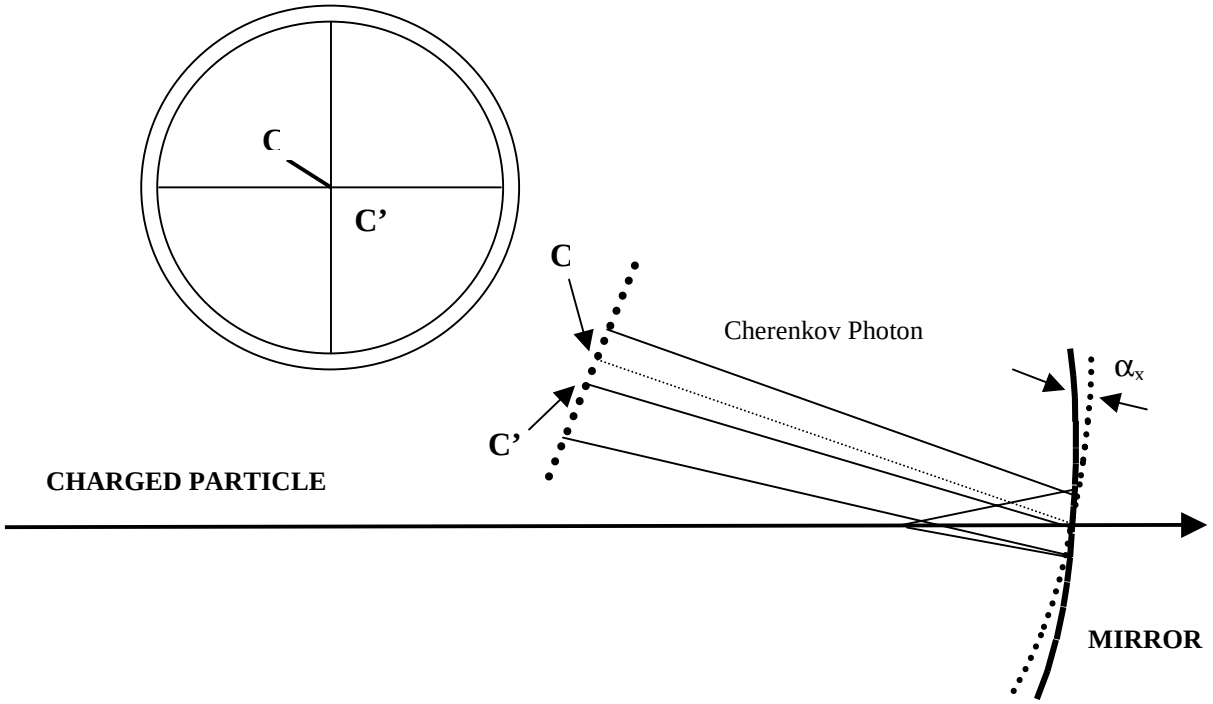

Figure 8: Reconstructed Cherenkov ring. C' is the centre of the reconstructed ring from a mirror with horizontal tilt α_x, while C is the expected centre of the ring if the mirror was perfectly aligned ($\alpha_x = 0$).

The positions and tilt angles of the mirror segments are displaced in such a manner that the difference in angle $\chi^2 = \Sigma(\theta_c^{rec} - \theta_c^{exp})^2/\sigma_c^2$, with σ_c the error in the Cherenkov angle, is minimised. One can only use tracks where the origin of the reflected photon in both planes of mirrors is unambiguous. A photon at the beginning of the radiator and another at the end of the radiator should reflect from the same pair of mirrors to be declared unambiguous. Depending on the momentum and the angle, between 5-10% of photons have an ambiguity in finding the mirror segments of origin. Once a subset of tracks with unambiguous mirror segment pairs has been found, the least-squares minimisation produces a set of linear equations that gives the tilts of the

spherical and plane mirrors. This procedure has to be iterated a number of times until the residuals in all mirror segments are minimised.

The conclusion in [13] suggests that if the relative alignment achieved by the surveyors in RICH 2 is ~0.5 mrad then a total alignment accuracy of 0.2 mrad (including mirror quality) can be achieved by performing the alignment with data. A similar conclusion was reached in [12], where a Cherenkov angle resolution of σ = 0.650 mrad was achieved, compared to an ideal resolution of σ = 0.630 mrad, which is due to all the other sources of error in the the measurement of the Cherenkov angle. This would suggest, subtracting both figures in quadrature, that an alignment error of 0.16 mrad had been achieved with this procedure.
Both studies suggest that a resolution of ~0.2 mrad can be achieved with this type of alignment technique, which would not be sufficient to achieve the experimental aim of 0.1 mrad in the alignment of RICH 2. In addition, this operation is complicated by the fact that one needs to align the two sets of mirrors simultaneously, which makes it difficult to monitor the alignment constants in real time, while the detector is taking data. Monitoring of the alignment can be achieved in real time with the help of an online laser alignment system, as proposed in the following section.

6.3 Laser Alignment System

The installation of a laser alignment system in both the RICH 1 and RICH 2 detectors would improve the prospects of achieving an accurate alignment for the following reasons:

1. It will be possible to perform a pre-alignment of the detectors with the laser system before the gas enclosures are closed off. This would allow one to verify the relative positioning of the mirrors and the photon detectors, as determined by the surveyors, before any gas is introduced into the gas enclosure, allowing one to make any corrections before the detectors are made inaccessible.

2. A laser alignment system can produce a series of discrete laser points that can be compared with their theoretical positions, which simplifies the analysis. The unambiguous nature of the laser points allows one to measure these at the photon detector plane and optimise the tilts and positions of the mirrors in real time.

3. A laser alignment system allows one to continue monitoring the positions of these laser points throughout data taking, thereby making allowances for thermal and vibrational corrections of the positions of the mirrors and photon detectors.

4. Such a laser alignment system is complementary to the final alignment with data, as was described in Section 6.2.

The main difficulties with any laser alignment system are how to introduce the laser points inside the detector volume and how to ensure that the alignment system itself is as stable as the detector. There are a number of ideas that can be used. We will enumerate some of these in the following paragraphs.

As was mentioned in Section 3, the multi-point alignment system of the ATLAS muon spectrometer [6-8] makes use of a silicon laser diode in combination with commercially available fibre splitters to feed an array of single mode optical fibres that deliver laser alignment references into their detector. The optic fibres with collimator optics produce a diffraction limited Gaussian laser beam with a 2-3 mm width over distances between 10-20 m [6]. These fibres with their collimating optics could be arranged in a matrix, supported by a light frame structure, in front of the spherical mirrors as shown in Figure 9 for the case of RICH 2. Such an array of fibres would only add minimally to the material budget inside the acceptance of the RICH detectors.

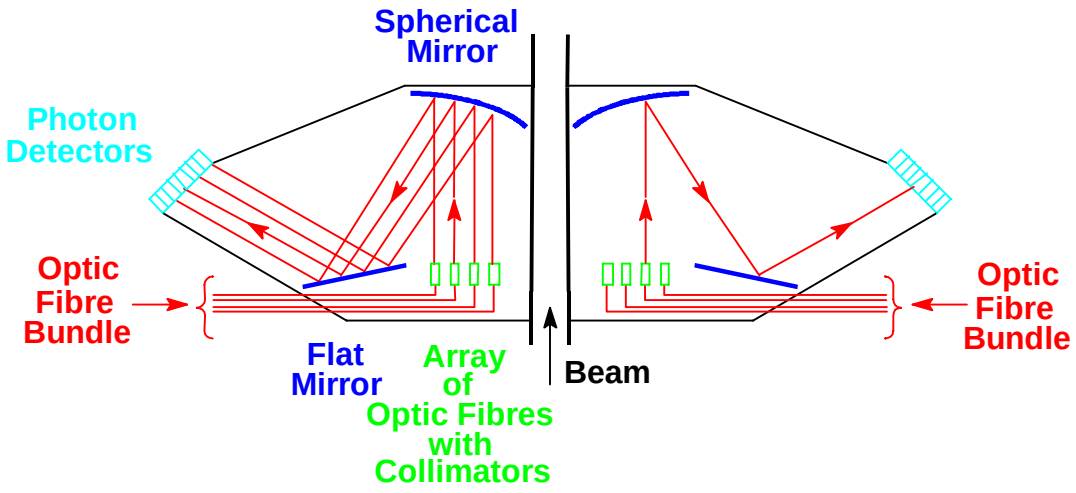

Figure 9: Optic fibre alignment system for RICH 2.

Alternatively, the fibres could be mounted on the spherical mirrors themselves, perpendicular to the mirror surface. Four laser points per mirror segment would allow redundancy in the positioning of each of the mirrors (Figure 10). This would simplify the optics, since one would not need to set-up a support structure for the fibres.

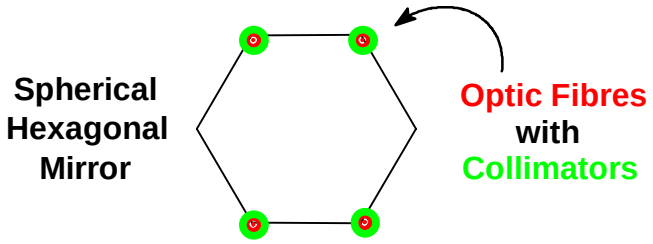

Figure 10: Four laser points per hexagonal mirror segment.

If the light beams from the fibres are not collimated enough to achieve the design resolution, alternatively one could inject a laser beam from the side and bounce the beam from an array of

semi-transparent mirrors (Figure 11). The semi-transparent mirrors would be mounted on a light frame in front of the first plane of spherical mirrors and the laser would be introduced into the chamber through small windows on the side of the gas enclosure.

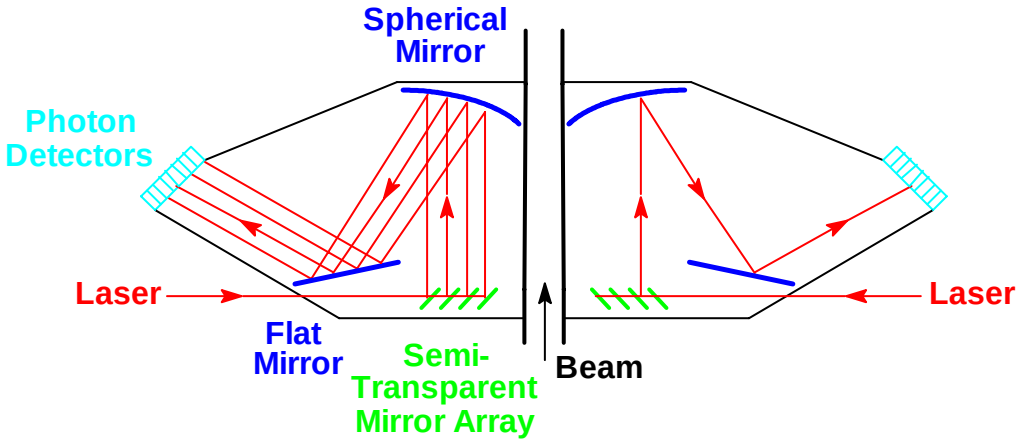

Figure 11: Laser alignment system with semi-transparent mirrors for RICH 2.

One final option would include the use of a mirror with a piezoelectric mount. Again, the laser light would be introduced from the side of the enclosure, and the piezoelectric mount can be used to scan the light across the face of the mirrors. Because of the mirror segmentation, the edges of the mirrors can be identified by the shadows that would be left from the reconstructed photons on the detector plane (Figure 12).

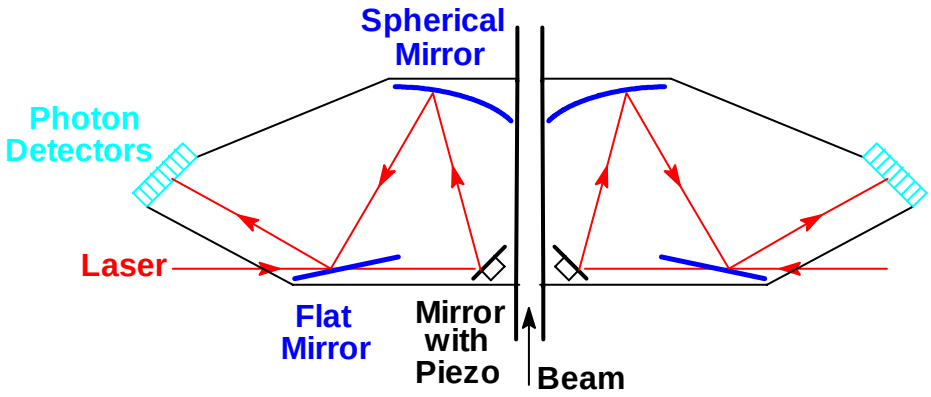

Figure 12: Laser alignment system with piezoelectric mirror mount.

All of these options should be studied in detail before adopting a final design. The final design would be the one that minimises the alignment error. Such a solution could be different for the RICH 1 and RICH 2 detectors, taking into account the different resolution requirements and the smaller availability of space in RICH 1. However, the possibility of having a laser alignment

system for both detectors, allows one to monitor the stability of the optical components in a simple and straightforward manner.

7. Control Hardware and Software

The control hardware and software of the RICH detectors will conform to the accepted format for the control systems of LHCb [14,15], which will be developed in the framework of the Joint Controls Project (JCOP) [16] in common with the other LHC experiments. The generic architecture for such a system is shown in Figure 13. The Experimental Control System (ECS) oversees the whole process and interfaces with the Detector Control System (DCS), the LHC machine information (LHC), the Data Acquisition (DAQ) and the Technical Support (TS) in the experimental hall. The DCS organizes the control flow between each of the sub-detector systems (DetDcsN). The RICH system control software would be one such system. Within the RICH detector control systems, there would be a number of subsystems (SubSysN), which could contain each of the devices (DevN) that need to be controlled, such as all the control devices that have been described in the present document.

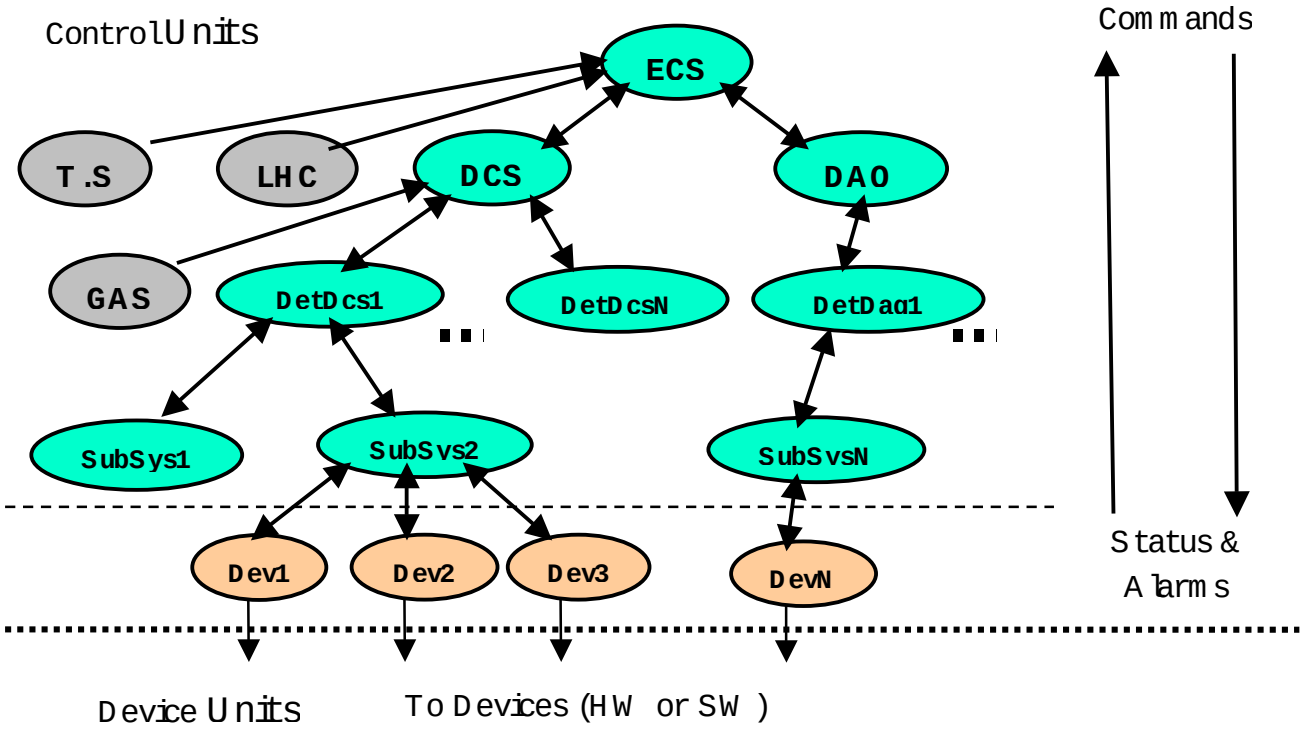

Figure 13: Generic architecture for the LHCb control systems.

A possible architecture for the hardware devices in charge of the experiment control systems is shown in Figure 14. A series of computers, within a Local Area Network (LAN) have responsibility for the supervision and data storage. Each of the supervisory computers are connected to the computers that are directly linked to the Programmable Logic Controllers (PLC) that are in charge of running each of the devices. Supervisory Control and Data Acquisition

(SCADA) software, which will be common to all LHC experiments[3], will be available on all machines. The SCADA systems will be versatile enough to allow the configuration of multiple device components (such as power supplies, PC interfaces, specific modules in electronic racks and crates, gas system, cooling, the LHC machine parameters, the LHCB magnet, etc.) running on a variety of data buses (such as CAN, PROFIBUS, WorldFip, …). Electronics board control interface solutions include the use of Smart Module "credit card PC" that allow one to control the electronics boards locally [17].

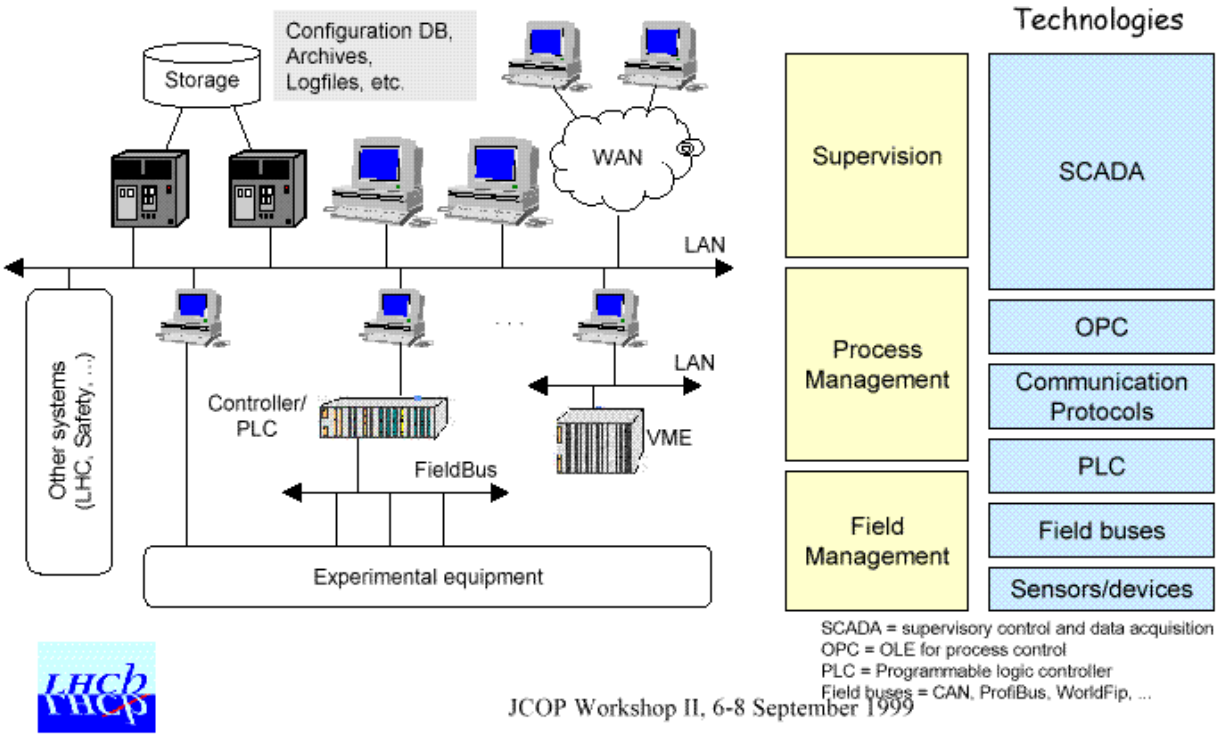

Figure 14: Hardware architecture for the experiment control supervisory systems.

There will be device user interfaces for each of the devices under control with the normal user tasks, such as monitoring certain parameters, alarm levels for the proper operation of the devices and the actions permitted by the users. Proper logging of the data will be carried out within this framework. A "partitioned" data model will allow relative autonomy amongst each of the control units, so as not to interfere with the general operation in case of problems and to allow local control which minimizes the network traffic.

The use of common hardware components and a common software control system amongst all the LHC experiments allows one to standardize solutions for common problems. The RICH control systems group will work in close collaboration with the Experiment Control Systems (ECS) group of LHCb and with JCOP to find common solutions for all the control demands of the LHCb RICH detectors.

[3] This will be a commercial tool that will be contracted out by a tendering process.

8. Conclusions

The present document is a first attempt at describing the physical quantities of the RICH detectors that need to be monitored and controlled to ensure that the performance of the RICH is maintained throughout the duration of the experimental program of LHCb.

The control of the gas re-circulation system of the RICH detectors was described initially, followed by possible devices that would monitor the refractive index of the gas (an ultrasonic sonar system and a Fabry-Perot interferometer). The transparency of the gas as a function of wavelength could be monitored with a monochromatic light source. The mechanical stability of the support structures can be monitored with an array of single mode fibers with collimating optics in combination with semi-transparent amorphous silicon sensors. Quantities that need to be monitored and controlled in the electronics systems have also been identified. The monitoring of the photon detector performance can be achieved with the aid of a light source that can identify dead and low efficiency channels.

The alignment of the RICH detector optics can be achieved as a three stage process:

1. Survey of the mirror and detector positions with the CERN based surveyors;
2. Use of a laser alignment system to verify the relative alignment of the photon detector and mirror components before the final sealing of the gas enclosure; and
3. Final alignment of the optical systems by reconstructing Cherenkov rings from ultra-relativistic particles.

In addition, the laser alignment system can be used to monitor in real time the stability of the optical components of the RICH detectors.

The control hardware and software of the LHCb RICH detectors will conform to the standard SCADA solutions that will be adopted by all LHC experiments, and LHCb in particular, in close collaboration with the CERN ECS team.

References

[1] M. Bosteels et al., “LHCb RICH Gas System proposal”, LHCb 2000-079.
[2] M.L. Andrieux et al., Nucl. Instr. and Meth. A 371 (1996) 259-262.
[3] E. Fokitis et al., Nucl. Phys. B (Proc. Suppl.) 44 (1995) 246-251.
[4] A. Filippas et al., Nucl. Instr. and Meth. A 371 (1996) 255-258.
[5] G. Lenzen et al., Nucl. Instr. and Meth. A 343 (1994) 268-272.
[6] H. Kroha, Nucl. Phys. B (Proc. Suppl.) 54 (1997) 80.
[7] W. Blum, H. Kroha, P. Widman, Nucl. Instr. and Meth. A 377 (1996) 404.
[8] W. Blum, H. Kroha, P. Widman, Nucl. Instr. and Meth. A 367 (1995) 413.
[9] G. Barichello et al., Nucl. Instr. and Meth. A 419 (1998) 1-15.
[10] J. Bibby, S. Wotton, “LHCb RICH Electronics - requirements, specifications and implementation”, LHCb 2000-074.

[11] LHCb Technical Proposal, The LHCb Collaboration, CERN/LHCC 98-4 (February 1998).
[12] A. Gorišek et al., Nucl. Instr. and Meth. A 433 (1999) 408-412.
[13] F. Filthaud, RICH meeting, 19 March 1999.
[14]. See for example, the Front End Electronics, Control and Data Acquisition Workshop, 16-19 May 2000, http://lhcb.cern.ch/computing/online/html/Workshop%20Agenda.htm
[15] C. Gaspar, "Experimental Control System, Architecture and Tools", talk given at [14], http://lhcb.cern.ch/computing/online/powerpoint/FE_DAQ_ECS_2000.ppt
[16] See: http://itcowww.cern.ch/jcop
[17] B. Jost, "Controls Interface to Electronics Boards (Credit-Card PC and Local Control Bus)", talk given at [14], http://lhcb.cern.ch/computing/online/powerpoint/board-level%20controls%20and%20local%20bus.ppt